Coupling Liquid Phases in 3D Condensates and 2D Membranes: Successes, Challenges, and Tools

Heidi M.J. Weakly & Sarah L. Keller*

Department of Chemistry, University of Washington – Seattle, Seattle, WA 98103 USA

Running title: Coupling lipid domains and condensates

Keywords: phase separation, liquid, membrane, condensate, membraneless organelle, lipid, wetting

* Corresponding author: slkeller@uw.edu

ORCID numbers:

H.M.J. Weakly	0000-0001-8594-6337
S.L. Keller	0000-0001-5919-0185

ABSTRACT:

This review describes the major experimental challenges researchers meet when attempting to couple phase separation between membranes and condensates. Although it is well known that phase separation in a 2D membrane should affect molecules capable of forming a 3D condensate (and vice versa), few researchers have quantified the effects to date. The scarcity of these measurements is not due to lack of intense interest or effort in the field. Rather, it reflects significant experimental challenges in manipulating coupled membranes and condensates to yield quantitative values. These challenges transcend many molecular details, which means they impact a wide range of systems. This review highlights recent exciting successes in the field, and it lays out a comprehensive list of tools that address potential pitfalls for researchers who are considering coupling membranes with condensates.

INTRODUCTION:

Organelles in cells are either bounded by a 2-dimensional (2D) membrane or are membraneless, 3-dimensional (3D) condensates. Membranes and condensates can both organize through liquid-liquid phase separation (LLPS), which can be crucial for cell viability. For example, during periods of nutrient stress, lipid membranes of yeast vacuoles phase separate into 2D domains (1–3) corresponding to liquid-ordered and liquid-disordered (Lo and Ld) phases in model membranes (2). These membrane transitions are reversible, and the domains can merge quickly, like liquids (4, 5). Likewise, stress granules, which are condensates enriched in RNA-binding proteins and mRNA, arise when cells experience stressors, including heat and pH (6, 7). Condensates can also merge quickly, like liquids rather than solids (8).

In some cases, membranes and condensates interact. Wetting of membranes by molecules found in condensates been implicated in crucial biological functions such as signal transduction pathways in T cells (9), tight junctions in endothelial cells (10), endocytic vesicles formation (11), and other processes (12–16). The biological importance of these phenomena has prompted researchers to investigate thermodynamically coupled systems of phase-separating membranes and phase-separating solutions.

Liquid-liquid phase separation has been widely reviewed for both 2D membranes (17–21) and 3D condensates (22–28). Given the rich literature about the conditions needed to achieve phase separation in both systems, it may seem surprising that few measurements quantifying effects of their coupling have been reported to date. This paucity is not due to researchers' lack of interest. Rather, it reflects significant experimental challenges that researchers have faced.

Our goal in this review is to help new researchers in the field quickly surmount challenges in coupling membranes to condensates. We will briefly introduce relevant terminology and theoretical concepts, then highlight recent groundbreaking measurements. We will then describe experimental challenges that researchers have faced and conclude with a list of techniques and molecular tools to mitigate the challenges.

SECTION I: Terminology and theoretical concepts of liquids on surfaces

Dewetting, partial wetting, and complete wetting reflect the strength of interactions between molecules in liquid droplets and surfaces (Fig. 1A). As an example, dewetting occurs when water beads on a hydrophobic surface. At the other extreme, wetting occurs when water completely covers a hydrophilic surface. Partial wetting is characterized by a contact angle between 0˚ (wetting) and 180˚ (dewetting); the "critical wetting point" occurs at the first nonzero contact angle (29). In the absence of a macroscopic droplet, interactions may be sufficient to create a molecularly thin film 2D surface phase of the same molecules found in liquid droplets, a phenomenon called "prewetting" (30–34). These concepts apply equally well when the droplet is a phase-separated fluid condensate and the surface is a membrane (Fig. 1B-C) (35, 36).

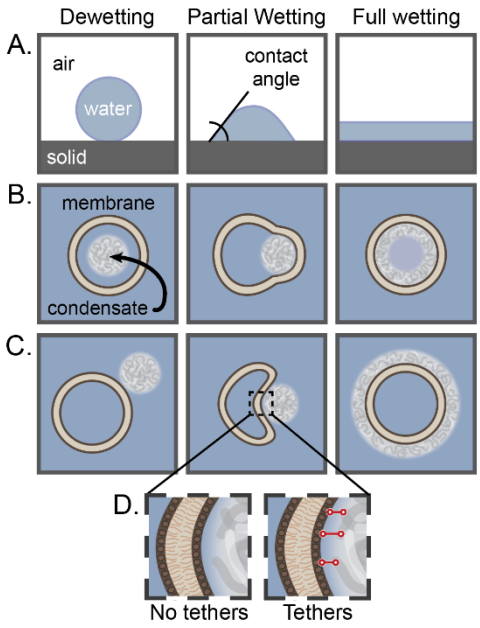

Figure 1: Schematic of dewetting, partial wetting, and complete wetting. (A) Liquid drops on solid surfaces. Liquid condensates (B) inside or (C) outside vesicle membranes, both (D) with and without tethers between lipid headgroups and molecules in the condensate.

SECTION II: Recent progress in experiment, theory, and simulation

To date, investigators have found two observables that can be used to provide insight into coupling between liquid phases of membranes and condensates: (1) changes in morphology and (2) shifts in phase boundaries, whether in concentration or miscibility transition temperature, T_{mix}.

Membranes bend easily

When vesicle membranes are in contact with phase-separated 3D fluids, they adopt a range of shapes (Fig. 1B–C and reviewed elsewhere (37–40)). When the membrane is also phase-separated, coupled phase separation can occur. Coupling can be facilitated by incorporating molecular tethers (discussed in detail in Tool 4) that link condensates to membranes (Fig. 1D). For example, when a phase-separating solution of polyethylene glycol (PEG) and dextran is encapsulated in a vesicle containing a small fraction of PEG-lipids (35), membrane domains enriched in PEG-lipids coat the solution phase enriched in PEG molecules. Subsequent fission of the vesicles results in two populations: one of which is enriched in PEG-lipids and encapsulates PEG molecules (35).

Membranes shift protein threshold concentrations

Condensates are dense clusters of biomolecules with reversible, multivalent interactions. Protein solutions demix into condensed and dilute phases when the protein concentration surpasses a threshold, sometimes called the “saturation concentration” (Fig. 2). When at least one protein in a condensate binds to a membrane, the concentration of condensate locally increases, so that condensate proteins prewet the membrane at lower concentrations than required for bulk condensates (Fig. 2) (41–43). For example, when Whi3 proteins, which are involved in RNA transcript regulation at the endoplasmic reticulum, are tethered to membranes, they form surface condensates at concentrations orders of magnitude lower than in solution (16). Similarly, the protein FtsZ, which is involved in cell division in *E. coli*, forms small condensates with the DNA-binding protein SlmA at a lipid interface (44). FtZ:SlmA surface condensates coalesce on shorter timescales, characteristic of liquid phases (44). Future work will undoubtedly demonstrate this concept with other proteins, where the importance of each system will lie in its cellular role.

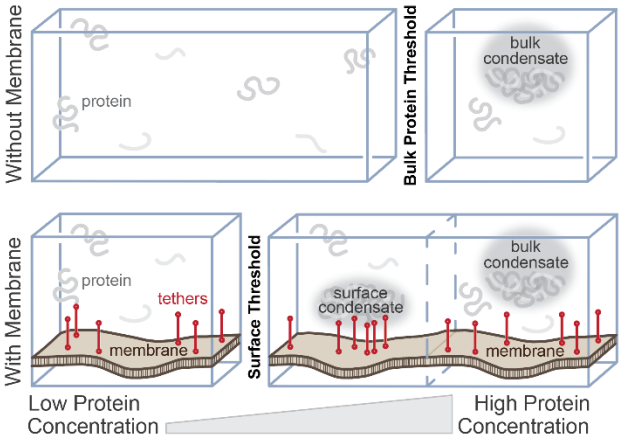

Figure 2: Surface condensates form at lower protein concentrations than bulk condensates. Top: At low concentrations, soluble proteins are in a uniform, dilute phase. As the protein concentration linearly increases above a bulk condensate threshold, a droplet of condensed protein phase coexists with the dilute protein solution. Bottom: If the protein binds to a membrane, whether via a tether or not, a molecularly-thin, 2D condensate consistent can prewet the surface at a lower concentration than the bulk threshold. The surface condensate alters the local distribution of tethers, but not their number. The bulk condensate threshold is unchanged by the presence of the membrane.

If condensate proteins are tethered to only *one* of the membrane phases, domain formation can further concentrate the proteins (45). Wang et al. found that low concentrations of pLAT proteins condensed on phase-separated membranes, whereas they do not form condensates on mixed membranes (45). Similarly, charged lipids that are highly enriched in one membrane phase can enable surface phases (46, 47). One example is the Noc condensate (a bacterial nucleoid occlusion protein complex), which is enhanced by high surface densities of negatively charged lipids (48).

Protein condensates shift membrane T_{mix}

Above a characteristic temperature, T_{mix}, membranes are uniform, whereas below T_{mix}, membrane lipids demix into coexisting liquid ordered (Lo) and liquid disordered (Ld) phases (Fig. 3). Given that T_{mix} increases when membrane components are crosslinked or accumulate in one phase (49–53), and that lipid packing can increase in membranes wet by condensates (54), T_{mix} should increase when 3D condensates couple to one membrane phase.

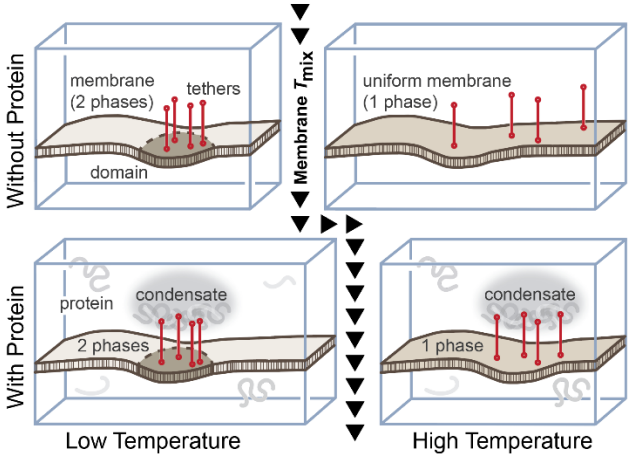

Figure 3: Protein condensates can shift the mixing temperature, T_{mix}, of lipid membranes to higher values. Top Row: At low temperatures, two liquid phases coexist in the membrane: the liquid ordered phase (Lo) and the liquid disordered phase (Ld). At high temperatures, the lipids mix in a single liquid phase. Bottom Row: Interactions between a protein condensate and lipids in only one membrane phase (either the Lo or the Ld phase) are predicted to increase the membrane's T_{mix}, independent of molecular details (33).

Indeed, Lee et al. found that more membranes phase separated when proteins were coupled to the membrane's Ld phase (55). Chung et al. achieved a breakthrough by quantifying a shift in T_{mix} (56). They found that coupling a condensate of the proteins LAT, Grb2 and SOS with model membranes increased T_{mix} (by 6°C for their specific membrane and solution conditions) (56). Wang et al. also quantified T_{mix} for a similar model system (45).

Tether density is a key parameter

In model membranes, increasing the coupling between condensates and membranes generally increases phase separation (57, 58). In simulations and theory (33, 34), coupling or tethering a dilute solution of phase-separable molecules to a membrane expands the prewetting regime. Rouches et al. found the prewetting regime increases further when the membrane is near a miscibility critical point (33). Integral membrane proteins may act as obstacles, further modulating condensate-molecule interactions and reducing effective tether densities (59).

One way to tune the coupling strength is to vary densities of molecules that tether the membrane to the condensate. Unfortunately, limited ranges of tether densities for measurements of T_{mix} are experimentally accessible. Above a certain membrane surface density, condensate molecules experience lateral steric pressure. This density is a function of

the molecules' molar mass (60, 61). Large molecules like PEG5000-DOPE can experience steric pressure at membrane concentrations of only 1-2 mol% (61).

In cells, interfering with molecular linkers between condensates and membranes can disrupt downstream signaling pathways. For example, decoupling LAT protein from membrane domains by mutating the transmembrane domain of LAT prevents LAT condensate formation and curtails downstream signaling events in T cells (45). Mutating LAT's transmembrane domain changes the partitioning of the condensate within the membrane, effectively lowering the local tether density. However, the specific molecular mechanisms by which de-coupling condensates from membranes domains interferes with signaling is not yet known.

SECTION III: Experimental challenges of characterizing phase-separation of membranes in contact with protein solutions

Four challenges that researchers encounter when attempting to measure T_{mix} of membranes in contact with protein and/or RNA solutions include: [1] aggregation of free-floating vesicles, [2] membrane tubulation, [3] difficulties in exchanging aqueous solutions, and [4] slow collective motion of lipids in membranes on solid surfaces.

Liquid-liquid phase separation in membranes is commonly imaged in ≥10 μm single-walled vesicles, in membranes on solid or polymer substrates, or in membranes spanning holes in supports (Fig. 4). These systems are called "giant unilamellar vesicles" (GUVs) (62), "supported lipid membranes" (SLBs) (63, 64), and "black lipid membranes" (BLMs) (65, 66), respectively. While experiments may be possible in all these systems, each has advantages and disadvantages.

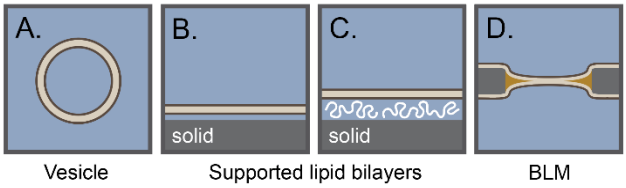

Figure 4: Schematics of four membrane configurations: (A) a giant unilamellar vesicle (GUV), (B) a supported lipid membrane (SLB) on a solid support, (C) a supported lipid membrane on a polymer support, and (D) a black lipid membrane (BLM) spanning solid supports coated with oil (orange wedges). In all panels, hydrophobic regions of the bilayer are light tan and lipid headgroups are dark brown."

For example, one feature of taut giant vesicles is that micron-sized domains can be imaged by standard fluorescence microscopy. Moreover, when phase-separable solutions are enclosed within vesicles, condensates are easily formed through changes in osmotic pressure (67) or pH (68). Challenges of free-floating vesicles include aggregation and shape changes, especially under conditions optimized for proteins.

Challenge 1: Aggregation of free-floating vesicles

Mixing vesicle solutions with condensate solutions can cause aggregation. Even simple salt-containing buffers can cause aggregation of lipid vesicles as shown in Fig. 5. Furthermore, when protein condensates bind to free-floating vesicles, condensates can bridge the gap between adjacent vesicles to create aggregates. Aggregation presents three disadvantages. First, imaging membrane domains on aggregated vesicles is difficult, especially when domains are small. The best method for imaging aggregated vesicles is confocal microscopy; however, these microscopes typically lack temperature control systems required to measure T_{mix}. Second, proteins' access to some membranes in the aggregate is hindered, leading to large variation in protein concentration across membrane surfaces. Third, when membranes adhere, ordered domains localize to the interfaces, and can appear at temperatures above T_{mix} of unadhered membranes (69, 70).

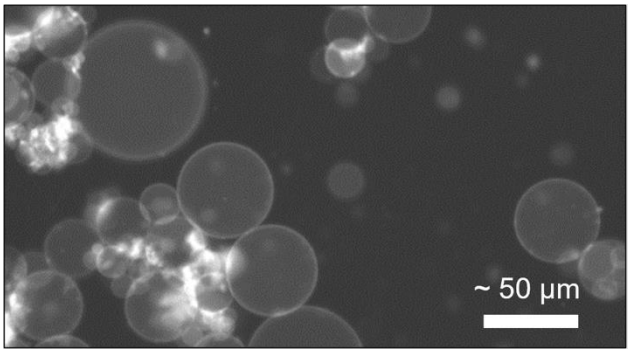

Figure 5: Lipid vesicles can aggregate in buffer. Here, vesicles are composed of 98 mol% di(18:1)PC and 2 mol% 18:1 DGS-NTA(Ni) (Avanti Polar Lipids) were produced by a standard electroformation technique (71) and then introduced to an osmotically-matched buffer of 25 mM HEPES and 150 mM NaCl. The image was collected by H.M.J.W. with a Nikon Eclipse ME600L upright epifluorescence microscope and a Hamamatsu C13440 camera.

Aggregation of vesicles is frequently mitigated by adding charged lipids or surfactants (72). However, at high salt concentrations the Debye length is shorter, reducing electrostatic repulsion between charged lipids. Adding a hydrophilic polymer such as PEG to lipid headgroups confers some steric repulsion, albeit at molecular length scales(73). If experiments can be completed quickly, it may be sufficient for vesicles to aggregate slowly, as when they are dilute in solution. Tactics to avoid membrane aggregation include immobilizing vesicles or directly assembling membranes on supports; advantages and caveats of which are discussed in Section IV.

Challenge 2: Membrane bending and tubulation

Tubules are common in membranes (Fig. 6), especially in vesicles with excess area (more membrane than necessary to enclose their volume) (74, 75), in supported membranes with area changes (76, 77), and in membranes that bind proteins (57, 78, 79). Tubules can also form in vesicles during gentle hydration (80) and electroformation (71, 80). In experiments that couple membranes to condensates, tubules complicate quantitative measurements. First, membrane phase separation is difficult to identify when domains nucleate in thin, undulating tubules. Second, tubulation can cause nonuniform lipid compositions (81). Third, confounding variables arise. For example, Ld phases appear in highly curved membranes of vesicles (82) and supported bilayers (83). Similarly, some proteins (e.g., the I-BAR protein IRSp53 (84)) preferentially partition onto tubules. Therefore, if condensate proteins interact with tubules of only one membrane phase, it is unclear if the interaction arises from the membrane's lipid composition or its shape.

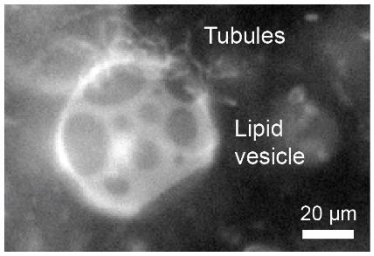

Figure 6: Membrane tubules can form at vesicle surfaces, complicating quantitative measurements of coupling between protein condensates and membranes. Fluorescence micrograph of thin, white, Ld-phase tubules protruding from a broad area at the top of the vesicle. The vesicle contains 31:31:35 mol% di(18:1)PC: di(16:0)PC:cholesterol with 2.2 mol% 18:0-PEG5000 PE (Avanti Polar Lipids) and 0.8% Texas Red PE (Thermo Fisher Scientific), in a hypertonic solution of sucrose at 33°C. The image was collected by H.M.J.W. on instrumentation described elsewhere (85). Contrast was enhanced to make dim tubules visible.

Membrane tubulation can be mitigated by membrane tension, typically applied through osmotic pressure gradients. However, tension can shift the membrane's miscibility temperature (86–89). Unfortunately, membrane tubulation can be *increased* by factors as benign as making membranes with different types of molecules (e.g., noncylindrical lipids (78, 90), charged lipids (91), or block copolymers (92)), applying gradients in temperature (93) or pH (94), introducing a plastic microbead (95), or establishing asymmetry in aqueous salt or sugar concentrations (96, 97). When vesicles encapsulate immiscible solutions, inward tubules can coat the interface between the two solutions, whether the solutions have few components (e.g., dextran and PEG (98)) or many (e.g., tonoplasts of *A. thaliana*) (38).

Tubulation is also driven by membrane asymmetry (74) in lipids (e.g., GM1 (99), DHA (100), cholesterol, or DOPC (76)), fatty acids (101), DNA origami (102, 103), peptides (104, 105), or proteins (78, 79, 106). Polypeptides with attractive domains, like FUSLC, generate inward tubules in vesicles, whereas repulsive protein domains generate outward tubules (107). Some proteins interact directly with membranes (e.g., N-BAR domains (79, 106)). Others may be tethered to the membrane and interact via steric crowding; smaller proteins produce membrane

tubes more frequently (78). Some tethered condensate proteins (the RGG domain of LAF-1, the low-complexity domain of FUS, and the low complexity domain of hnRNPA2) form molecularly thin, liquid domains on membranes and cause tubulation (57). Higher densities of tethers cause more tubules (57, 78). Testing prewetting theories (33) by varying tether densities becomes challenging when broad ranges of tether densities become inaccessible due to tubulation.

Challenge 3: Difficulties in exchanging solutions

Condensate proteins are typically added to phase-separated membranes by solution exchange. However, fluid flow can push free-floating giant (>10 μm) vesicles out of the field of view, even when they have sunk in lower density solutions. To address this problem, membranes can be tethered to surfaces, discussed further in Tool 3. Vesicles can also be deposited in flow cells, captured in microfluidic wells, or trapped behind partitions (53, 75, 108, 109). One caveat is that trapped vesicles often touch a solid surface, which can cause phase-separated domains to reorganize, even when the surface is passivated with BSA proteins or when the membrane's temperature is above its miscibility transition (69, 110, 111). An alternative trapping method places neutrally buoyant vesicles in a dead-end microfluidic channel while a solution flows past the channel's entrance (112).

Challenge 4: Slow collective motion of lipids in membranes on solid surfaces

Depositing lipid membranes on surfaces solves many challenges, especially if the surface fits inside a low-volume flow cell. However, hydrodynamic theory suggests that if the aqueous layer between the membrane and surface is too thin, then lipid domains cannot form (or grow by colliding and coalescing (113)) on experimental timescales (114). As a result, the domains are typically noncircular and can be too small to resolve by fluorescence microscopy (115, 116). Although circular, micron-scale liquid domains sometimes form in membranes deposited directly on clean glass, they are immobile, and their thermal history may be important (116, 117).

SECTION IV. TOOLS AND METHODS

Tool 1: Black Lipid Membranes

Black lipid membranes (BLMs, Fig. 4D), which span holes in supports, have several advantages for coupling condensates to membranes. Because both sides of the membrane are in contact with thick water layers, round, micron-scale liquid domains form on experimental timescales. BLMs are compatible with fluid exchange. When proteins are introduced to both sides of the membrane, transmembrane coupling of proteins is possible (41). Even when proteins are introduced to only one side, membrane tension prevents tubulation (41).

BLMs that span large (micron-scale) distances are typically formed by one of four methods:

1) An oil droplet containing lipids is "painted" over a hole in a plastic sheet or microfluidic device(118, 119). A lipid bilayer forms as oil drains to the hole's perimeter, where oil bridges the molecular thickness of the membrane and the macroscopic thickness of the plastic.

2) A Transmission Electron Microscopy (TEM) grid with an array of holes is coated with an oil layer containing lipids by moving the grid from an oily solution into an aqueous solution (66). Bilayers form as oil drains to the perimeters of the holes. A challenge is that the volume of oil must be optimized for each lipid composition (66).

3) In the Montal-Mueller technique (65), lipid monolayers at air-water interfaces are passed over a hole in a hydrophobic, plastic sheet pre-coated with long-chain oils. The oil at the perimeter of the bilayer and any oil molecules that persist within the bilayer do not alter its miscibility transition temperature or the areas of the two phases (120). An advantage of Montal-Mueller membranes is that each monolayer leaflet can contain a different ratio of lipids: these asymmetric bilayers have opened new avenues for probing transbilayer coupling of liquid phases (120). Disadvantages are that the method is challenging and that volumes are large (~1 mL), so temperature changes slowly.

4) In modified Montal-Mueller techniques, lipid monolayers at two oil-water interfaces assemble into a bilayer. These bilayers are called various names (including contacting monolayers (121) and droplet interface bilayers (122)), and they may contain nm-scale decane inclusions (123). In one technique (124), phase-separating membranes can span very large areas (~1 mm^2, Fig. 7).

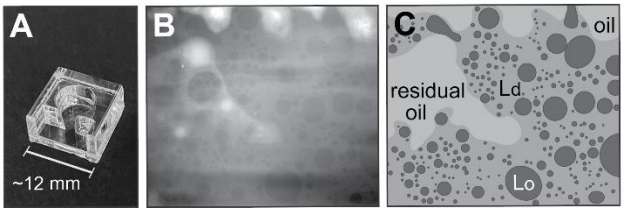

Figure 7: Coexisting Lo and Ld phases can be imaged in black lipid membranes. (A) Custom chamber of laser-cut acrylic by Dave Richmond and Dan Fletcher (125). Vertical black lipid membranes form across the gap between the rectangular and circular wells. (B) Fluorescence micrograph of a membrane spanning ~1 mm (the image width). The membrane contains the lipids di(18:1)PC, di(16:0)PC, and cholesterol, and was imaged by Dave Richmond and S.L.K. (C) Schematic of Panel B, identifying Lo/Ld membrane phases. In the micrograph, excess oil has not entirely drained to the hole's perimeter.

Tool 2: Stacked and cushioned membranes

Membranes can be offset from solid supports by stacking membranes or assembling them on polymer cushions. Controls may be needed to account for higher transition temperatures in SLBs (126), especially on inhomogeneous surfaces (127), with respect to vesicles.

1) Stacked membranes

Membranes can be stacked by bursting a GUV on a membrane supported on a solid substrate. The upper membrane may be separated from the lower membrane by a uniformly thin layer of water or by a thick water pocket (115); both present advantages and disadvantages. If the upper membrane lies flat, binding of proteins can cause it to roll and delaminate; similar changes in spontaneous curvature cause tubulation(128). Affixing the upper membrane to the lower

membrane (e.g., via DNA binding) leads to other problems: the upper membrane can disintegrate within hours unless it contains high ratios of saturated lipids(129, 130). If there is a water pocket, domains in the upper membrane may diffuse or may be immobilized by membrane deformations, which are enhanced by protein binding(131).

An alternative method of generating membrane stacks is to spin-coat lipids on a substrate such as mica(63) and erode the resulting multilayer with a jet of water(132). In regions where only two stacked membranes remain, domains in the upper membrane have some attributes of GUV domains: liquid domains deform due to fluid flow, become round in tens of seconds, grow to be tens of microns by Ostwald ripening, and occasionally coalesce(132). Stacks of phase-separating membranes are also made by hydrating dry lipids on a silicon substrate(133).

2) Membranes cushioned by polymer headgroups and/or substrates

Lipopolymers (lipids with polymer head groups) can offset membranes in which they reside from solid substrates. Because polymer lengths can be varied, the distance and interaction between the membrane and support can be tuned. Membranes separated from glass supports by PEGylated fatty acids can grow to be micron-scale but are thereafter stationary and/or noncircular on experimental timescales(134). Other headgroup modifications include poly(2-oxazoline) polymers(135) and oligopeptides(136).

Another strategy is to coat supports with polymers before depositing membranes. For example, polydimethylsiloxane (PDMS) is easily patterned with microstructures to test the impact of curvature on domain formation(83, 137). The PDMS surface must be hydrophilic; otherwise, cholesterol can leach into it from the membrane(138). Membrane domains on PDMS or other stiff cushions (e.g., cellulose) can be stationary on experimental timescales(139).

When the two strategies are combined (membranes contain lipopolymer headgroups and rest on PDMS surfaces), micron-scale, circular, liquid domains form in membranes cooled very slowly through T_{mix}, at ~0.04 ºC/min(140). A challenge is that these domains are also stationary on experimental timescales(140).

Tool 3: Membrane-substrate tethers

To mitigate aggregation of free-floating vesicles and their displacement by fluid flow, vesicles can be attached to substrates via molecular tethers. A typical approach is to coat the substrate with a functionalized polymer such as PEG-biotin, followed by the addition of an avidin, which binds biotinylated lipids anchored in the membrane(141–143). Optimizing the tether concentration is important: giant vesicles with high tether densities deform such that large areas are in contact with the substrate, leading to domain reorganization(110). This adhesion can be reduced by incorporating a co-polymer like PEG-silane or PLL-g-PEG at the interface(144, 145).

Alternative tethers use DNA-lipids(146), which are well suited for ~100 nm vesicles. However, as with other tethers, high concentrations of DNA-lipids cause giant vesicles to rupture, forming patches on glass and SLB supports(130). However, when too few tethers are deployed, lipid anchors pull out of giant vesicles when flow is introduced. Another alternative is to use electroformed vesicles that are still tethered to their conductive substrates by tubules that withstand slow exchange of solutions(147). However, these vesicles often touch, and quantification of the total membrane area is difficult.

Tool 4: Tethers to couple condensates to membranes

To couple phase separation in condensates and membranes, the two systems must be in contact. One option is to link condensates to membranes via tethers (Fig. 1D), which include histidine-binding lipids, phosphoinositide lipids, polymer-based linkers, lipid-DNA linkers, and biotinylated lipids.

In the literature, "tethers" include molecules that bind membranes to substrates (see *Tool 3*). Some molecules can be used for both purposes, although membrane-substrate tethers are often designed to bind irreversibly under experimental conditions, whereas membrane-condensate interactions should be reversible. One clever approach is to tether only one protein of a multi-component condensate to the membrane and then introduce remaining proteins in solution(55, 56). Tethers enable strong controls that distinguish effects of localizing a protein on a membrane and adding more proteins to form a condensate(55, 56) or that distinguish effects of attaching condensate molecules to immobile versus mobile tethers(16). In turn, new controls are warranted. For example, Cans et al.(67) attribute increases in membrane T_{mix} to the addition of PEG-lipid tethers and to encapsulation of a solution of PEG and dextran in vesicles. Similarly, membrane T_{mix} can shift when tethers bind multiple lipids (as streptavidin with biotinylated lipids, or choleratoxin with GM1-lipids)(49). Most tethers strongly partition into either the Lo or Ld membrane phase, which likely also shifts T_{mix}.

Histidine-binding lipids

Polyhistidine tags (His-tags) are sequences of 2-6 histidines attached to proteins, commonly used to purify them via affinity chromatography(148). The tags can also link proteins to membranes via phospholipids with nickel- or copper-chelating headgroups (e.g., NTA(Ni) or IDA(Cu)). Metal-chelating tethers have two advantages. First, binding of his-tagged proteins to lipids is reversible upon addition of EDTA at low concentrations(149). Second, the tethers can preferentially partition to the Lo or Ld phase of membranes, depending on the length and saturation of their lipid tails(85).

A disadvantage of metal-chelating lipid tethers is their high melting temperatures. For instance, lipids with IDA (iminodiacetic acid) headgroups and 16:0 carbon chains melt at 55˚C (73˚C in the presence of Cu^{2+}). As a result, binary membranes of this lipid and a low melting lipid (e.g., POPC) demix into gel and liquid phases at room temperature(78, 149). Also, metal-chelating tethers are incompatible with thiol compounds, which disrupt links between His-tagged proteins and NTA(Ni) lipids(150). This impedes super-resolution imaging techniques, which frequently use thiols to enable fluorophore photoswitching. Similarly, if aqueous solutions require oxygen scavenging systems with glucose, it is important to run controls that measure how glucose affects phase separation of condensates(150).

Phosphoinositides

Negatively charged phosphoinositide (PI) lipids are found in membranes of eukaryotic cells, including the endoplasmic reticulum, endosomes, and plasma membranes. Although PI-lipids are low abundance, they are important because of the specificity with which several proteins

bind to them(151), making PIs a convenient tether to protein condensates. One such protein, N-WASP, has been used to anchor actin networks to membranes containing a fluorescently labeled PIP_2-lipid (di(16:0)-TMR-PIP_2) that preferentially partitioned to the Ld phase (53). Challenges of PI-lipids are that they may cluster if buffers contain divalent cations(152, 153), they are difficult to incorporate in model membranes at concentrations above a few mole percent(152), and they can leach from membranes to form micelles in solution(154).

PEG-lipids

Pegylated lipids (PEG-lipids) can directly couple membranes to phase-separating solutions of PEG and dextran(35, 67, 155) or can behave as a tether when modified with functional groups like biotin. At low concentrations of PEG-lipids, their partitioning between membrane phases is influenced by the lipid tails, the length of the polymer, and the hydrophobicity of the functional group[13]. At higher concentrations set by the PEG-lipids' molar mass, steric interactions can drive PEG-lipids from domains(61). At membrane concentrations of PEG(2000)-lipid above ~10 mol%, vesicles break up into membrane discs(157).

DNA-lipids

Liquid-liquid phase separation has been implicated in organization(158, 159) and repair of DNA(160, 161). DNA strands attached to lipid headgroups can interact with biocondensates by binding to complement strands, interacting with DNA-binding proteins, or folding into aptamers that bind other molecules. For short strands, hybridization can be reversed by increasing temperature. DNA strands are typically anchored to the membrane by one or more sterols. By modifying the number of sterols, replacing cholesterol with tocopherol, or replacing model membranes with giant plasma membrane vesicles, the partitioning of DNA-lipids can be tuned between the Lo and Ld phases(162–164).

Biotinylated lipids

Biotin and avidin proteins bind with high affinity ($K_d \sim 10^{-15}$ M)(165). Biotin conjugated to the headgroup of phospholipids is frequently used to facilitate protein-membrane interactions. A caveat is that vesicles that contain biotinylated lipids can be crosslinked by avidin (which contains four binding sites for biotin) and form multi-vesicle aggregates. Vesicles can be redispersed by adding soluble biotin, which has a higher affinity than biotinylated lipids for avidin(166, 167). Some researchers incorporate a third molecule that reversibly interacts with a membrane or condensate, such as a biotinylated DNA oligonucleotide(16).

If proximity between a lipid and its biotin label is a concern, polyethylene glycol can be inserted as a spacer, as in biotin-PEG-lipids. A caveat is that the spacer length (and the mole fraction of biotin-PEG-lipid in the membrane) affects the partitioning of biotin-PEG-lipids between membrane phases(168).

Tool 5: Compatible proteins

Tools 1-4 focused on membrane components. Which corresponding protein systems should researchers choose? The PhaSepBD database contains thousands of entries(169), but will any protein system that undergoes phase separation suffice?

The phase behavior and molecular interactions of condensates are reviewed elsewhere(22, 39, 170). In brief, condensate molecules that are primarily polar and charged are described by Flory-Huggins theory for enthalpically driven phase separation. Above an upper critical temperature or upon addition of salt, entropic forces overcome chain-chain interactions and the system ceases to phase separate. In contrast, condensate molecules that are primarily hydrophobic, such as elastin-like polypeptides, have lower critical temperatures above which interactions between the peptides and solvent are disfavored, and the system phase separates(170).

The ideal choice of proteins depends on the experimental design. For example, if salt will be added to affect protein phase separation, the proteins should be charged and potential effects of salt on membrane phase separation should also be considered(46, 47). Similarly, if temperature will be varied to affect membrane phase separation, the potential effects of protein interactions and denaturation should be considered (Fig. 8). Molecules that may tolerate higher temperatures include engineered peptides(171) or a polymeric systems(172). An alternative tactic is to choose membranes that demix at lower temperatures(45).

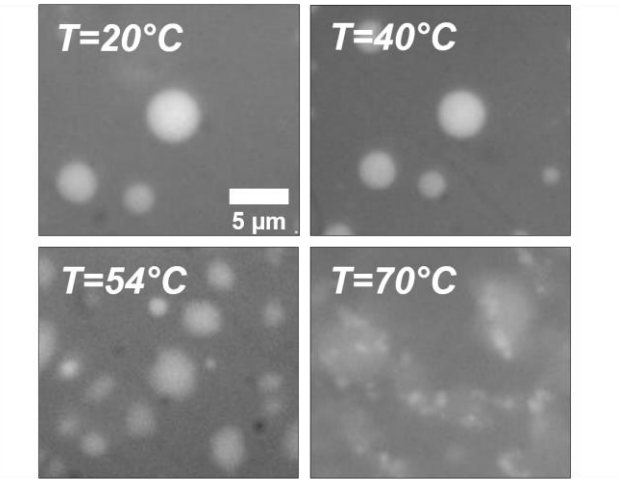

Figure 8. Condensates can destabilize as temperature increases. Representative fluorescence micrographs of solutions of 25 µM MBP-$(SH_3)_5$-His, 37.5 µM $(PRM)_5$, 25 mM HEPES, and 150 mM NaCl after mixing 2 hr at room temperature. At low temperatures, the condensates form spherical droplets with sharp edges, characteristic of liquid-liquid phase separation (20°C and 40°C). At higher temperatures, the edges of the condensates blur, their shapes become nonspherical, and bright puncta appear throughout the solution (54°C and 70°C). This behavior cannot be explained by shape fluctuations near a critical point and may reflect protein denaturation. The proteins were produced and purified by Michael Cotten and Michael Rosen; solutions were mixed and imaged by H.M.J.W.

Several researchers have leveraged protein systems known to cluster on membranes. For example, condensates of the linker for the activation of T cells (LAT) and its binding partners

(Grb2 and Sos1) have been employed to shift membrane miscibility temperatures(45, 56). Another protein system in use is Nephrin and its cytoplasmic binding partners (Nck and N-WASP)(42, 171).

CONCLUSION

In conclusion, quantitative experiments that couple lipid membranes and protein condensates require clever design choices. Here, we have reviewed several challenges that arise in the experiments, as well as several tools that mitigate the challenges. Using these tools, researchers have made recent, exciting successes in observing thermodynamic changes in coupled systems, including shifts in membrane transition temperatures and the formation of surface condensates. We expect to see additional advances in the future, especially in research that combines theory and modelling to support quantitative experiments that characterize surface phases under prewetting conditions.

ABBREVIATIONS

2D = 2-dimensional

3D = 3-dimensional

BLM = black lipid membrane

GUV = giant unilamellar vesicle

IDA = iminodiacetic acid

NTA = nitrilotriacetic acid

LLPS = liquid-liquid phase separation

PDMS = polydimethylsiloxane

PEG = polyethylene glycol

PI = phosphatidylinositol

PIP_2 = phosphatidylinositol 4,5-bisphosphate

PIP_3 = phosphatidylinositol 3,4,5-trisphosphate

SLB = supported lipid bilayer

T_{mix} = miscibility transition temperature

TEM = transmission electron microscopy

ACKNOWLEDGEMENTS

We thank Michael Rosen and Michael Cotten for producing phase-separable proteins. We thank Dave Richmond and Dan Fletcher for their collaboration in proof-of-concept experiments with

black lipid membranes. We thank Aurelia Honerkamp-Smith, Ilya Levental, Kandice Levental, Darryl Sasaki, Jeanne Stachowiak, and Sarah Veatch for advice and encouragement. HMJW was supported by the National Institute of General Medical Sciences of the National Institutes of Health under Award Number T32GM008268. This research was supported by National Science Foundation grant MCB-1925731 and MCB-2325819 to SLK.

DECLARATION OF INTERESTS

The authors declare no competing interests.

REFERENCES

1. Moeller, C.H., and W.W. Thomson. 1979. An ultrastructural study of the yeast tonoplast during the shift from exponential to stationary phase. *J. Ultrastruct. Res.* 68:28–37.

2. Toulmay, A., and W.A. Prinz. 2013. Direct imaging reveals stable, micrometer-scale lipid domains that segregate proteins in live cells. *J. Cell Biol.* 202:35–44.

3. Wang, C.-W., Y.-H. Miao, and Y.-S. Chang. 2014. A sterol-enriched vacuolar microdomain mediates stationary phase lipophagy in budding yeast. *J. Cell Biol.* 206:357–366.

4. Rayermann, S.P., G.E. Rayermann, C.E. Cornell, A.J. Merz, and S.L. Keller. 2017. Hallmarks of Reversible Separation of Living, Unperturbed Cell Membranes into Two Liquid Phases. *Biophys. J.* 113:2425–2432.

5. Leveille, C.L., C.E. Cornell, A.J. Merz, and S.L. Keller. 2022. Yeast cells actively tune their membranes to phase separate at temperatures that scale with growth temperatures. *Proc. Natl. Acad. Sci.* 119:e2116007119.

6. Molliex, A., J. Temirov, J. Lee, M. Coughlin, A.P. Kanagaraj, H.J. Kim, T. Mittag, and J.P. Taylor. 2015. Phase Separation by Low Complexity Domains Promotes Stress Granule Assembly and Drives Pathological Fibrillization. *Cell*. 163:123–133.

7. Riback, J.A., C.D. Katanski, J.L. Kear-Scott, E.V. Pilipenko, A.E. Rojek, T.R. Sosnick, and D.A. Drummond. 2017. Stress-Triggered Phase Separation Is an Adaptive, Evolutionarily Tuned Response. *Cell*. 168:1028-1040.e19.

8. Kroschwald, S., S. Maharana, D. Mateju, L. Malinovska, E. Nüske, I. Poser, D. Richter, and S. Alberti. 2015. Promiscuous interactions and protein disaggregases determine the material state of stress-inducible RNP granules. *eLife*. 4:e06807.

9. Su, X., J.A. Ditlev, E. Hui, W. Xing, S. Banjade, J. Okrut, D.S. King, J. Taunton, M.K. Rosen, and R.D. Vale. 2016. Phase separation of signaling molecules promotes T cell receptor signal transduction. *Science*. 352:595–599.

10. Beutel, O., R. Maraspini, K. Pombo-García, C. Martin-Lemaitre, and A. Honigmann. 2019. Phase Separation of Zonula Occludens Proteins Drives Formation of Tight Junctions. *Cell*. 179:923-936.e11.

11. Day, K.J., G. Kago, L. Wang, J.B. Richter, C.C. Hayden, E.M. Lafer, and J.C. Stachowiak. 2021. Liquid-like protein interactions catalyse assembly of endocytic vesicles. *Nat. Cell Biol.* 23:366–376.

12. Ma, W., and C. Mayr. 2018. A Membraneless Organelle Associated with the Endoplasmic Reticulum Enables 3′UTR-Mediated Protein-Protein Interactions. *Cell*. 175:1492-1506.e19.

13. Lee, J.E., P.I. Cathey, H. Wu, R. Parker, and G.K. Voeltz. 2020. Endoplasmic reticulum contact sites regulate the dynamics of membraneless organelles. *Science*. 367:eaay7108.

14. Yu, X., L. Zhang, J. Shen, Y. Zhai, Q. Jiang, M. Yi, X. Deng, Z. Ruan, R. Fang, Z. Chen, X. Ning, and Z. Jiang. 2021. The STING phase-separator suppresses innate immune signalling. *Nat. Cell Biol.* 23:330–340.

15. Bergeron-Sandoval, L.-P., S. Kumar, H.K. Heris, C.L.A. Chang, C.E. Cornell, S.L. Keller, P. François, A.G. Hendricks, A.J. Ehrlicher, R.V. Pappu, and S.W. Michnick. 2021. Endocytic proteins with prion-like domains form viscoelastic condensates that enable membrane remodeling. *Proc. Natl. Acad. Sci.* 118:e2113789118.

16. Snead, W.T., A.P. Jalihal, T.M. Gerbich, I. Seim, Z. Hu, and A.S. Gladfelter. 2022. Membrane surfaces regulate assembly of ribonucleoprotein condensates. *Nat. Cell Biol.* 24:461–470.

17. Veatch, S.L., and S.L. Keller. 2005. Seeing spots: Complex phase behavior in simple membranes. *Biochim. Biophys. Acta*. 1746:172–185.

18. Sengupta, P., B. Baird, and D. Holowka. 2007. Lipid rafts, fluid/fluid phase separation, and their relevance to plasma membrane structure and function. *Semin. Cell Dev. Biol.* 18:583–590.

19. Marsh, D. 2009. Cholesterol-induced fluid membrane domains: A compendium of lipid-raft ternary phase diagrams. *Biochim. Biophys. Acta*. 1788:2114–2123.

20. Honerkamp-Smith, A.R., S.L. Veatch, and S.L. Keller. 2009. An introduction to critical points for biophysicists; observations of compositional heterogeneity in lipid membranes. *Biochim. Biophys. Acta*. 1788:53–63.

21. Heberle, F.A., and G.W. Feigenson. 2011. Phase Separation in Lipid Membranes. *Cold Spring Harb. Perspect. Biol.* 3:a004630.

22. Brangwynne, C.P., P. Tompa, and R.V. Pappu. 2015. Polymer physics of intracellular phase transitions. *Nat. Phys.* 11:899–904.

23. Banani, S.F., H.O. Lee, A.A. Hyman, and M.K. Rosen. 2017. Biomolecular condensates: organizers of cellular biochemistry. *Nat. Rev. Mol. Cell Biol.* 18:285–298.

24. Alberti, S. 2017. The wisdom of crowds: regulating cell function through condensed states of living matter. *J. Cell Sci.* 130:2789–2796.

25. Posey, A.E., A.S. Holehouse, and R.V. Pappu. 2018. Phase Separation of Intrinsically Disordered Proteins. *Methods Enzymol.* 611:1–30.

26. Langdon, E.M., and A.S. Gladfelter. 2018. A New Lens for RNA Localization: Liquid-Liquid Phase Separation. *Annu. Rev. Microbiol.* 72:255–271.

27. Bracha, D., M.T. Walls, and C.P. Brangwynne. 2019. Probing and engineering liquid-phase organelles. *Nat. Biotechnol.* 37:1435–1445.

28. Hirose, T., K. Ninomiya, S. Nakagawa, and T. Yamazaki. 2023. A guide to membraneless organelles and their various roles in gene regulation. *Nat. Rev. Mol. Cell Biol.* 24:288–304.

29. Moldover, M.R., and J.W. Cahn. 1980. An Interface Phase Transition: Complete to Partial Wetting. *Science*. 207:1073–1075.

30. Ebner, C., and W.F. Saam. 1977. New Phase-Transition Phenomena in Thin Argon Films. *Phys. Rev. Lett.* 38:1486–1489.

31. Nakanishi, H., and M.E. Fisher. 1982. Multicriticality of Wetting, Prewetting, and Surface Transitions. *Phys. Rev. Lett.* 49:1565–1568.

32. de Gennes, P.G. 1985. Wetting: statics and dynamics. *Rev Mod Phys*. 57:827–863.

33. Rouches, M., S.L. Veatch, and B.B. Machta. 2021. Surface densities prewet a near-critical membrane. *Proc. Natl. Acad. Sci.* 118:e2103401118.

34. Zhao, X., G. Bartolucci, A. Honigmann, F. Jülicher, and C.A. Weber. 2021. Thermodynamics of wetting, prewetting and surface phase transitions with surface binding. *New J. Phys.* 23:123003.

35. Helfrich, M.R., L.K. Mangeney-Slavin, M.S. Long, K.Y. Djoko, and C.D. Keating. 2002. Aqueous Phase Separation in Giant Vesicles. *J. Am. Chem. Soc.* 124:13374–13375.

36. Li, Y., R. Lipowsky, and R. Dimova. 2008. Transition from Complete to Partial Wetting within Membrane Compartments. *J. Am. Chem. Soc.* 130:12252–12253.

37. Lipowsky, R. 2018. Response of Membranes and Vesicles to Capillary Forces Arising from Aqueous Two-Phase Systems and Water-in-Water Droplets. *J. Phys. Chem. B*. 122:3572–3586.

38. Kusumaatmaja, H., A.I. May, M. Feeney, J.F. McKenna, N. Mizushima, L. Frigerio, and R.L. Knorr. 2021. Wetting of phase-separated droplets on plant vacuole membranes leads to a competition between tonoplast budding and nanotube formation. *Proc. Natl. Acad. Sci.* 118:e2024109118.

39. Botterbusch, S., and T. Baumgart. 2021. Interactions between Phase-Separated Liquids and Membrane Surfaces. *Appl. Sci.* 11:1288.

40. Mangiarotti, A., N. Chen, Z. Zhao, R. Lipowsky, and R. Dimova. 2023. Wetting and complex remodeling of membranes by biomolecular condensates. *Nat. Commun.* 14:2809.

41. Lee, Y., S. Park, F. Yuan, C.C. Hayden, S.Q. Choi, and J.C. Stachowiak. 2022. Lateral compression of lipids drives transbilayer coupling of liquid-like protein condensates. 2022.12.21.521462.

42. Banjade, S., and M.K. Rosen. 2014. Phase transitions of multivalent proteins can promote clustering of membrane receptors. *eLife*.

43. Sun, D., X. Zhao, T. Wiegand, G. Bartolucci, C. Martin-Lemaitre, S.W. Grill, A.A. Hyman, C. Weber, and A. Honigmann. 2023. Assembly of tight junction belts by surface condensation and actin elongation. 2023.06.24.546380.

44. Paccione, G., M.Á. Robles-Ramos, C. Alfonso, M. Sobrinos-Sanguino, W. Margolin, S. Zorrilla, B. Monterroso, and G. Rivas. 2022. Lipid Surfaces and Glutamate Anions Enhance Formation of Dynamic Biomolecular Condensates Containing Bacterial Cell Division Protein FtsZ and Its DNA-Bound Regulator SlmA. *Biochemistry*. 61:2482–2489.

45. Wang, H.-Y., S.H. Chan, S. Dey, I. Castello-Serrano, J.A. Ditlev, M.K. Rosen, K.R. Levental, and I. Levental. 2023. Coupling of protein condensates to ordered lipid domains determines functional membrane organization. *Sci. Adv.* 9.

46. Vequi-Suplicy, C.C., K.A. Riske, R.L. Knorr, and R. Dimova. 2010. Vesicles with charged domains. *Biochim. Biophys. Acta*. 1798:1338–1347.

47. Blosser, M.C., J.B. Starr, C.W. Turtle, J. Ashcraft, and S.L. Keller. 2013. Minimal effect of lipid charge on membrane miscibility phase behavior in three ternary systems. *Biophys. J.* 104:2629–2638.

48. Babl, L., A. Merino-Salomón, N. Kanwa, and P. Schwille. 2022. Membrane mediated phase separation of the bacterial nucleoid occlusion protein Noc. *Sci. Rep.* 12:17949.

49. Hammond, A.T., F.A. Heberle, T. Baumgart, D. Holowka, B. Baird, and G.W. Feigenson. 2005. Crosslinking a lipid raft component triggers liquid ordered-liquid disordered phase separation in model plasma membranes. *Proc. Natl. Acad. Sci.* 102:6320–6325.

50. Machta, B.B., E. Gray, M. Nouri, N.L.C. McCarthy, E.M. Gray, A.L. Miller, N.J. Brooks, and S.L. Veatch. 2016. Conditions that Stabilize Membrane Domains Also Antagonize n-Alcohol Anesthesia. *Biophys. J.* 111:537–545.

51. Cornell, C.E., N.L.C. McCarthy, K.R. Levental, I. Levental, N.J. Brooks, and S.L. Keller. 2017. n-Alcohol Length Governs Shift in Lo-Ld Mixing Temperatures in Synthetic and Cell-Derived Membranes. *Biophys. J.* 113:1200–1211.

52. Leung, S.S.W., and J. Thewalt. 2017. Link between Fluorescent Probe Partitioning and Molecular Order of Liquid Ordered-Liquid Disordered Membranes. *J. Phys. Chem. B*. 121:1176–1185.

53. Liu, A.P., and D.A. Fletcher. 2006. Actin Polymerization Serves as a Membrane Domain Switch in Model Lipid Bilayers. *Biophys. J.* 91:4064–4070.

54. Mangiarotti, A., M. Siri, N. Tam, Z. Zhao, L. Malacrida, and R. Dimova. 2023. Biomolecular condensates modulate membrane lipid packing and hydration. 2023.01.04.522768.

55. Lee, I.-H., M.Y. Imanaka, E.H. Modahl, and A.P. Torres-Ocampo. 2019. Lipid Raft Phase Modulation by Membrane-Anchored Proteins with Inherent Phase Separation Properties. *ACS Omega*. 4:6551–6559.

56. Chung, J.K., W.Y.C. Huang, C.B. Carbone, L.M. Nocka, A.N. Parikh, R.D. Vale, and J.T. Groves. 2021. Coupled membrane lipid miscibility and phosphotyrosine-driven protein condensation phase transitions. *Biophys. J.* 120:1257.

57. Yuan, F., H. Alimohamadi, B. Bakka, A.N. Trementozzi, K.J. Day, N.L. Fawzi, P. Rangamani, and J.C. Stachowiak. 2021. Membrane bending by protein phase separation. *Proc. Natl. Acad. Sci.* 118.

58. Ureña, J., A. Knight, and I.-H. Lee. 2022. Membrane Cargo Density-Dependent Interaction between Protein and Lipid Domains on the Giant Unilamellar Vesicles. *Langmuir*. 38:4702–4712.

59. Liu, Z., A. Yethiraj, and Q. Cui. 2023. Sensitive and selective polymer condensation at membrane surface driven by positive co-operativity. *Proc. Natl. Acad. Sci.* 120:e2212516120.

60. Scheve, C.S., P.A. Gonzales, N. Momin, and J.C. Stachowiak. 2013. Steric Pressure between Membrane-Bound Proteins Opposes Lipid Phase Separation. *J. Am. Chem. Soc.* 135:1185–1188.

61. Imam, Z.I., L.E. Kenyon, A. Carrillo, I. Espinoza, F. Nagib, and J.C. Stachowiak. 2016. Steric pressure among membrane-bound polymers opposes lipid phase separation. *Langmuir*. 32:3774–3784.

62. Dimova, R., and C. Marques. 2019. The Giant Vesicle Book. CRC Press, Taylor & Francis Group.

63. Mennicke, U., and T. Salditt. 2002. Preparation of solid-supported lipid bilayers by spin-coating. *Langmuir*. 18:8172–8177.

64. Lenz, P., C.M. Ajo-Franklin, and S.G. Boxer. 2004. Patterned supported lipid bilayers and monolayers on poly(dimethylsiloxane). *Langmuir*. 20:11092–11099.

65. Montal, M., and P. Mueller. 1972. Formation of Bimolecular Membranes from Lipid Monolayers and a Study of Their Electrical Properties. *Proc. Natl. Acad. Sci.* 69:3561–3566.

66. Lee, H.-R., Y. Lee, S.S. Oh, and S.Q. Choi. 2020. Ultra-Stable Freestanding Lipid Membrane Array: Direct Visualization of Dynamic Membrane Remodeling with

Cholesterol Transport and Enzymatic Reactions. *Small Weinh. Bergstr. Ger.* 16:e2002541.

67. Cans, A.-S., M. Andes-Koback, and C.D. Keating. 2008. Positioning Lipid Membrane Domains in Giant Vesicles by Micro-organization of Aqueous Cytoplasm Mimic. *J. Am. Chem. Soc.* 130:7400–7406.

68. Love, C., J. Steinkühler, D.T. Gonzales, N. Yandrapalli, T. Robinson, R. Dimova, and T.-Y.D. Tang. 2020. Reversible pH-Responsive Coacervate Formation in Lipid Vesicles Activates Dormant Enzymatic Reactions. *Angew. Chem. Int. Ed.* 59:5950–5957.

69. Zhao, J., J. Wu, and S.L. Veatch. 2013. Adhesion Stabilizes Robust Lipid Heterogeneity in Supercritical Membranes at Physiological Temperature. *Biophys. J.* 104:825–834.

70. Gordon, V.D., M. Deserno, C.M.J. Andrew, S.U. Egelhaaf, and W.C.K. Poon. 2008. Adhesion promotes phase separation in mixed-lipid membranes. *Europhys. Lett.* 84:48003.

71. Veatch, S.L. 2007. Electro-formation and fluorescence microscopy of giant vesicles with coexisting liquid phases. *Methods Mol. Biol. Clifton NJ*. 398:59–72.

72. Souza, T.P. de, G.V. Bossa, P. Stano, F. Steiniger, S. May, P.L. Luisi, and A. Fahr. 2017. Vesicle aggregates as a model for primitive cellular assemblies. *Phys. Chem. Chem. Phys.* 19:20082–20092.

73. Hui, S.W., T.L. Kuhl, Y.Q. Guo, and J. Israelachvili. 1999. Use of poly(ethylene glycol) to control cell aggregation and fusion. *Colloids Surf. B Biointerfaces*. 14:213–222.

74. Lipowsky, R. 2012. Spontaneous tubulation of membranes and vesicles reveals membrane tension generated by spontaneous curvature. *Faraday Discuss.* 161:305–331.

75. Bhatia, T., T. Robinson, and R. Dimova. 2020. Membrane permeability to water measured by microfluidic trapping of giant vesicles. *Soft Matter*. 16:7359–7369.

76. Rahimi, M., D. Regan, M. Arroyo, A.B. Subramaniam, H.A. Stone, and M. Staykova. 2016. Shape Transformations of Lipid Bilayers Following Rapid Cholesterol Uptake. *Biophys. J.* 111:2651–2657.

77. Staykova, M., D.P. Holmes, C. Read, and H.A. Stone. 2011. Mechanics of surface area regulation in cells examined with confined lipid membranes. *Proc. Natl. Acad. Sci. U. S. A.* 108:9084–9088.

78. Stachowiak, J.C., C.C. Hayden, and D.Y. Sasaki. 2010. Steric confinement of proteins on lipid membranes can drive curvature and tubulation. *Proc. Natl. Acad. Sci. U. S. A.* 107:7781–7786.

79. Sorre, B., A. Callan-Jones, J. Manzi, B. Goud, J. Prost, P. Bassereau, and A. Roux. 2012. Nature of curvature coupling of amphiphysin with membranes depends on its bound density. *Proc. Natl. Acad. Sci.* 109:173–178.

80. Rodriguez, N., F. Pincet, and S. Cribier. 2005. Giant vesicles formed by gentle hydration and electroformation: A comparison by fluorescence microscopy. *Colloids Surf. B Biointerfaces*. 42:125–130.

81. Roux, A., D. Cuvelier, P. Nassoy, J. Prost, P. Bassereau, and B. Goud. 2005. Role of curvature and phase transition in lipid sorting and fission of membrane tubules. *EMBO J.* 24:1537–1545.

82. Heinrich, M., A. Tian, C. Esposito, and T. Baumgart. 2010. Dynamic sorting of lipids and proteins in membrane tubes with a moving phase boundary. *Proc. Natl. Acad. Sci.* 107:7208–7213.

83. Parthasarathy, R., C.H. Yu, and J.T. Groves. 2006. Curvature-modulated phase separation in lipid bilayer membranes. *Langmuir*. 22:5095–5099.

84. Prévost, C., H. Zhao, J. Manzi, E. Lemichez, P. Lappalainen, A. Callan-Jones, and P. Bassereau. 2015. IRSp53 senses negative membrane curvature and phase separates along membrane tubules. *Nat. Commun.* 6:8529.

85. Cornell, C.E., A. Mileant, N. Thakkar, K.K. Lee, and S.L. Keller. 2020. Direct imaging of liquid domains in membranes by cryo-electron tomography. *Proc. Natl. Acad. Sci.* 117:19713–19719.

86. Portet, T., S.E. Gordon, and S.L. Keller. 2012. Increasing Membrane Tension Decreases Miscibility Temperatures; an Experimental Demonstration via Micropipette Aspiration. *Biophys. J.* 103:L35–L37.

87. Ayuyan, A.G., and F.S. Cohen. 2008. Raft Composition at Physiological Temperature and pH in the Absence of Detergents. *Biophys. J.* 94:2654–2666.

88. Hamada, T., Y. Kishimoto, T. Nagasaki, and M. Takagi. 2011. Lateral phase separation in tense membranes. *Soft Matter*. 7:9061–9068.

89. Oglęcka, K., P. Rangamani, B. Liedberg, R.S. Kraut, and A.N. Parikh. 2014. Oscillatory phase separation in giant lipid vesicles induced by transmembrane osmotic differentials. *eLife*. 3:e03695.

90. Sakuma, Y., T. Taniguchi, T. Kawakatsu, and M. Imai. 2013. Tubular Membrane Formation of Binary Giant Unilamellar Vesicles Composed of Cylinder and Inverse-Cone-Shaped Lipids. *Biophys. J.* 105:2074–2081.

91. Steinkühler, J., P. De Tillieux, R.L. Knorr, R. Lipowsky, and R. Dimova. 2018. Charged giant unilamellar vesicles prepared by electroformation exhibit nanotubes and transbilayer lipid asymmetry. *Sci. Rep.* 8:11838.

92. Lim, S.K., P. Rangamani, M. Nallani, A.S.W. Wong, H.-P.M. de Hoog, A.N. Parikh, M. Nallani, Sandin, Sara, and Liedberg, Bo. 2017. Spontaneous formation of nanometer scale tubular vesicles in aqueous mixtures of lipid and block copolymer amphiphiles. *Soft Matter*. 13:1107–1115.

93. Talbot, E.L., J. Kotar, L.D. Michele, and P. Cicuta. 2019. Directed tubule growth from giant unilamellar vesicles in a thermal gradient. *Soft Matter*. 15:1676–1683.

94. Khalifat, N., M. Rahimi, A.-F. Bitbol, M. Seigneuret, J.-B. Fournier, N. Puff, M. Arroyo, and M.I. Angelova. 2014. Interplay of Packing and Flip-flop in Local Bilayer Deformation. How Phosphatidylglycerol Could Rescue Mitochondrial Function in a Cardiolipin-deficient Yeast Mutant. *Biophys. J.* 107:879–890.

95. van der Wel, C., D. Heinrich, and D.J. Kraft. 2017. Microparticle Assembly Pathways on Lipid Membranes. *Biophys. J.* 113:1037–1046.

96. Karimi, M., J. Steinkühler, D. Roy, R. Dasgupta, R. Lipowsky, and R. Dimova. 2018. Asymmetric Ionic Conditions Generate Large Membrane Curvatures. *Nano Lett.* 18:7816–7821.

97. Schenk, N.A., P.J. Dahl, M.G. Hanna, A. Audhya, G.G. Tall, J.D. Knight, and A. Anantharam. 2018. A simple supported tubulated bilayer system for evaluating protein-mediated membrane remodeling. *Chem. Phys. Lipids*. 215:18–28.

98. Liu, Y., J. Agudo-Canalejo, A. Grafmüller, R. Dimova, and R. Lipowsky. 2016. Patterns of Flexible Nanotubes Formed by Liquid-Ordered and Liquid-Disordered Membranes. *ACS Nano*. 10:463–474.

99. Dasgupta, R., M.S. Miettinen, N. Fricke, R. Lipowsky, and R. Dimova. 2018. The glycolipid GM1 reshapes asymmetric biomembranes and giant vesicles by curvature generation. *Proc. Natl. Acad. Sci.* 115:5756–5761.

100. Thid, D., J.J. Benkoski, S. Svedhem, B. Kasemo, and J. Gold. 2007. DHA-induced changes of supported lipid membrane morphology. *Langmuir ACS J. Surf. Colloids*. 23:5878–5881.

101. Yoon, B.K., J.A. Jackman, M.C. Kim, and N.-J. Cho. 2015. Spectrum of Membrane Morphological Responses to Antibacterial Fatty Acids and Related Surfactants. *Langmuir*. 31:10223–10232.

102. Franquelim, H.G., A. Khmelinskaia, J.-P. Sobczak, H. Dietz, and P. Schwille. 2018. Membrane sculpting by curved DNA origami scaffolds. *Nat. Commun.* 9:811.

103. Franquelim, H.G., H. Dietz, and P. Schwille. 2021. Reversible membrane deformations by straight DNA origami filaments. *Soft Matter*. 17:276–287.

104. Domanov, Y.A., and P.K.J. Kinnunen. 2006. Antimicrobial Peptides Temporins B and L Induce Formation of Tubular Lipid Protrusions from Supported Phospholipid Bilayers. *Biophys. J.* 91:4427–4439.

105. Arouri, A., V. Kiessling, L. Tamm, M. Dathe, and A. Blume. 2011. Morphological Changes Induced by the Action of Antimicrobial Peptides on Supported Lipid Bilayers. *J. Phys. Chem. B*. 115:158–167.

106. Snead, W.T., W.F. Zeno, G. Kago, R.W. Perkins, J.B. Richter, C. Zhao, E.M. Lafer, and J.C. Stachowiak. 2018. BAR scaffolds drive membrane fission by crowding disordered domains. *J. Cell Biol.* 218:664–682.

107. Yuan, F., C.T. Lee, A. Sangani, J.R. Houser, L. Wang, E.M. Lafer, P. Rangamani, and J.C. Stachowiak. 2023. The ins and outs of membrane bending by intrinsically disordered proteins. *Sci. Adv.* 9:eadg3485.

108. Yamada, A., S. Lee, P. Bassereau, and C.N. Baroud. 2014. Trapping and release of giant unilamellar vesicles in microfluidic wells. *Soft Matter*. 10:5878–5885.

109. Robinson, T. 2019. Microfluidic Handling and Analysis of Giant Vesicles for Use as Artificial Cells: A Review. *Adv. Biosyst.* 3:e1800318.

110. Sarmento, M.J., M. Prieto, and F. Fernandes. 2012. Reorganization of lipid domain distribution in giant unilamellar vesicles upon immobilization with different membrane tethers. *Biochim. Biophys. Acta*. 1818:2605–2615.

111. Robinson, T., and P.S. Dittrich. 2019. Observations of Membrane Domain Reorganization in Mechanically Compressed Artificial Cells. *ChemBioChem*. 20:2666–2673.

112. Steinkühler, J., R.L. Knorr, Z. Zhao, T. Bhatia, S.M. Bartelt, S. Wegner, R. Dimova, and R. Lipowsky. 2020. Controlled division of cell-sized vesicles by low densities of membrane-bound proteins. *Nat. Commun.* 11:905.

113. Stanich, C.A., A.R. Honerkamp-Smith, G.G. Putzel, C.S. Warth, A.K. Lamprecht, P. Mandal, E. Mann, T.-A.D. Hua, and S.L. Keller. 2013. Coarsening Dynamics of Domains in Lipid Membranes. *Biophys. J.* 105:444–454.

114. Stone, H.A., and A. Ajdari. 1998. Hydrodynamics of particles embedded in a flat surfactant layer overlying a subphase of finite depth. *J. Fluid Mech.* 369:151–173.

115. Kaizuka, Y., and J.T. Groves. 2004. Structure and Dynamics of Supported Intermembrane Junctions. *Biophys. J.* 86:905–912.

116. Stottrup, B.L., S.L. Veatch, and S.L. Keller. 2004. Nonequilibrium Behavior in Supported Lipid Membranes Containing Cholesterol. *Biophys. J.* 86:2942–2950.

117. Seu, K.J., A.P. Pandey, F. Haque, E.A. Proctor, A.E. Ribbe, and J.S. Hovis. 2007. Effect of Surface Treatment on Diffusion and Domain Formation in Supported Lipid Bilayers. *Biophys. J.* 92:2445–2450.

118. Honigmann, A., C. Walter, F. Erdmann, C. Eggeling, and R. Wagner. 2010. Characterization of horizontal lipid bilayers as a model system to study lipid phase separation. *Biophys. J.* 98:2886–2894.

119. Samsonov, A.V., I. Mihalyov, and F.S. Cohen. 2001. Characterization of cholesterol-sphingomyelin domains and their dynamics in bilayer membranes. *Biophys. J.* 81:1486–1500.

120. Collins, M.D., and S.L. Keller. 2008. Tuning lipid mixtures to induce or suppress domain formation across leaflets of unsupported asymmetric bilayers. *Proc. Natl. Acad. Sci.* 105:124–128.

121. Funakoshi, K., H. Suzuki, and S. Takeuchi. 2006. Lipid Bilayer Formation by Contacting Monolayers in a Microfluidic Device for Membrane Protein Analysis. *Anal. Chem.* 78:8169–8174.

122. Danial, J.S.H., B. Cronin, C. Mallik, and M.I. Walllace. 2017. On demand modulation of lipid composition in an individual bilayer. *Soft Matter*. 13:1788–1793.

123. Kirchner, S.R., A. Ohlinger, T. Pfeiffer, A.S. Urban, F.D. Stefani, A. Deak, A.A. Lutich, and J. Feldmann. 2012. Membrane composition of jetted lipid vesicles: a Raman spectroscopy study. *J. Biophotonics*. 5:40–46.

124. Stachowiak, J.C., D.L. Richmond, T.H. Li, A.P. Liu, S.H. Parekh, and D.A. Fletcher. 2008. Unilamellar vesicle formation and encapsulation by microfluidic jetting. *Proc. Natl. Acad. Sci.* 105:4697–4702.

125. Richmond, D.L., E.M. Schmid, S. Martens, J.C. Stachowiak, N. Liska, and D.A. Fletcher. 2011. Forming giant vesicles with controlled membrane composition, asymmetry, and contents. *Proc. Natl. Acad. Sci.* 108:9431–9436.

126. Gunderson, R.S., and A.R. Honerkamp-Smith. 2018. Liquid-liquid phase transition temperatures increase when lipid bilayers are supported on glass. *Biochim. Biophys. Acta*. 1860:1965–1971.

127. Subramaniam, A.B., G. Guidotti, V.N. Manoharan, and H.A. Stone. 2013. Glycans pattern the phase behaviour of lipid membranes. *Nat. Mater.* 12:128–133.

128. Klenow, M.B., J.C. Jeppesen, and A.C. Simonsen. 2020. Membrane rolling induced by bacterial toxins. *Soft Matter*. 16:1614–1626.

129. Chung, M., R.D. Lowe, Y.H.M. Chan, P.V. Ganesan, and S.G. Boxer. 2009. DNA-tethered membranes formed by giant vesicle rupture. *J. Struct. Biol.* 168:190–199.

130. Chung, M., and S.G. Boxer. 2011. Stability of DNA-Tethered Lipid Membranes with Mobile Tethers. *Langmuir*. 27:5492–5497.

131. Kaizuka, Y., and J.T. Groves. 2010. Bending-mediated superstructural organizations in phase-separated lipid membranes. *New J. Phys.* 12:095001.

132. Jensen, M.H., E.J. Morris, and A.C. Simonsen. 2007. Domain Shapes, Coarsening, and Random Patterns in Ternary Membranes. *Langmuir*. 23:8135–8141.

133. Yokota, K., A. Toyoki, K. Yamazaki, and T. Ogino. 2014. Behavior of raft-like domain in stacked structures of ternary lipid bilayers prepared by self-spreading method. *Jpn. J. Appl. Phys.* 53:05FA11.

134. Roder, F., O. Birkholz, O. Beutel, D. Paterok, and J. Piehler. 2013. Spatial Organization of Lipid Phases in Micropatterned Polymer-Supported Membranes. *J. Am. Chem. Soc.* 135:1189–1192.

135. Purrucker, O., A. Förtig, R. Jordan, and M. Tanaka. 2004. Supported Membranes with Well-Defined Polymer Tethers—Incorporation of Cell Receptors. *ChemPhysChem*. 5:327–335.

136. Bunjes, N., E.K. Schmidt, A. Jonczyk, F. Rippmann, D. Beyer, H. Ringsdorf, P. Gräber, W. Knoll, and R. Naumann. 1997. Thiopeptide-Supported Lipid Layers on Solid Substrates. *Langmuir*. 13:6188–6194.

137. Subramaniam, A.B., S. Lecuyer, K.S. Ramamurthi, R. Losick, and H.A. Stone. 2010. Particle/Fluid Interface Replication as a Means of Producing Topographically Patterned Polydimethylsiloxane Surfaces for Deposition of Lipid Bilayers. *Adv. Mater.* 22:2142–2147.

138. Miller, E.J., K. Voïtchovsky, and M. Staykova. 2018. Substrate-led cholesterol extraction from supported lipid membranes. *Nanoscale*. 10:16332–16342.

139. Feriani, L., L. Cristofolini, and P. Cicuta. 2015. Soft pinning of liquid domains on topographical hemispherical caps. *Chem. Phys. Lipids*. 185:78–87.

140. Rinaldin, M., S.L.D. ten Haaf, E.J. Vegter, C. van der Wel, P. Fonda, L. Giomi, and D.J. Kraft. 2021. Supported lipid membranes with designed geometry. .

141. Yoon, T.-Y., B. Okumus, F. Zhang, Y.-K. Shin, and T. Ha. 2006. Multiple intermediates in SNARE-induced membrane fusion. *Proc. Natl. Acad. Sci.* 103:19731–19736.

142. Runas, K.A., and N. Malmstadt. 2014. Low levels of lipid oxidation radically increase the passive permeability of lipid bilayers. *Soft Matter*. 11:499–505.

143. Litz, J.P., N. Thakkar, T. Portet, and S.L. Keller. 2016. Depletion with Cyclodextrin Reveals Two Populations of Cholesterol in Model Lipid Membranes. *Biophys. J.* 110:635–645.

144. Bendix, P.M., M.S. Pedersen, and D. Stamou. 2009. Quantification of nano-scale intermembrane contact areas by using fluorescence resonance energy transfer. *Proc. Natl. Acad. Sci.* 106:12341–12346.

145. Runas, K.A., S.J. Acharya, J.J. Schmidt, and N. Malmstadt. 2016. Addition of Cleaved Tail Fragments during Lipid Oxidation Stabilizes Membrane Permeability Behavior. *Langmuir*. 32:779–786.

146. Ajo-Franklin, C.M., C. Yoshina-Ishii, and S.G. Boxer. 2005. Probing the Structure of Supported Membranes and Tethered Oligonucleotides by Fluorescence Interference Contrast Microscopy. *Langmuir*. 21:4976–4983.

147. Estes, D.J., and M. Mayer. 2005. Giant liposomes in physiological buffer using electroformation in a flow chamber. *Biochim. Biophys. Acta*. 1712:152–160.

148. Knecht, S., D. Ricklin, A.N. Eberle, and B. Ernst. 2009. Oligohis-tags: mechanisms of binding to Ni2+-NTA surfaces. *J. Mol. Recognit.* 22:270–279.

149. Hayden, C.C., J.S. Hwang, E.A. Abate, M.S. Kent, and D.Y. Sasaki. 2009. Directed Formation of Lipid Membrane Microdomains as High Affinity Sites for His-Tagged Proteins. *J. Am. Chem. Soc.* 131:8728–8729.

150. Feng, Z., X. Chen, X. Wu, and M. Zhang. 2019. Formation of biological condensates via phase separation: Characteristics, analytical methods, and physiological implications. *J. Biol. Chem.* 294:14823–14835.

151. Yu, J.W., J.M. Mendrola, A. Audhya, S. Singh, D. Keleti, D.B. DeWald, D. Murray, S.D. Emr, and M.A. Lemmon. 2004. Genome-Wide Analysis of Membrane Targeting by S. cerevisiae Pleckstrin Homology Domains. *Mol. Cell*. 13:677–688.

152. Carvalho, K., L. Ramos, C. Roy, and C. Picart. 2008. Giant Unilamellar Vesicles Containing Phosphatidylinositol(4,5)bisphosphate: Characterization and Functionality. *Biophys. J.* 95:4348–4360.

153. Wang, Y.-H., A. Collins, L. Guo, K.B. Smith-Dupont, F. Gai, T. Svitkina, and P.A. Janmey. 2012. Divalent Cation-Induced Cluster Formation by Polyphosphoinositides in Model Membranes. *J. Am. Chem. Soc.* 134:3387–3395.

154. Shukla, S., R. Jin, J. Robustelli, Z.E. Zimmerman, and T. Baumgart. 2019. PIP2 Reshapes Membranes through Asymmetric Desorption. *Biophys. J.* 117:962–974.

155. Long, M.S., C.D. Jones, M.R. Helfrich, L.K. Mangeney-Slavin, and C.D. Keating. 2005. Dynamic microcompartmentation in synthetic cells. *Proc. Natl. Acad. Sci. U. S. A.* 102:5920–5925.

156. Bordovsky, S.S., C.S. Wong, G.D. Bachand, J.C. Stachowiak, and D.Y. Sasaki. 2016. Engineering Lipid Structure for Recognition of the Liquid Ordered Membrane Phase. *Langmuir*. 32:12527–12533.

157. Edwards, K., M. Johnsson, G. Karlsson, and M. Silvander. 1997. Effect of polyethyleneglycol-phospholipids on aggregate structure in preparations of small unilamellar liposomes. *Biophys. J.* 73:258–266.

158. Larson, A.G., D. Elnatan, M.M. Keenen, M.J. Trnka, J.B. Johnston, A.L. Burlingame, D.A. Agard, S. Redding, and G.J. Narlikar. 2017. Liquid droplet formation by HP1α suggests a role for phase separation in heterochromatin. *Nature*. 547:236–240.

159. Strom, A.R., A.V. Emelyanov, M. Mir, D.V. Fyodorov, X. Darzacq, and G.H. Karpen. 2017. Phase separation drives heterochromatin domain formation. *Nature*. 547:241–245.

160. Oshidari, R., R. Huang, M. Medghalchi, E.Y.W. Tse, N. Ashgriz, H.O. Lee, H. Wyatt, and K. Mekhail. 2020. DNA repair by Rad52 liquid droplets. *Nat. Commun.* 11:695.

161. Kilic, S., A. Lezaja, M. Gatti, E. Bianco, J. Michelena, R. Imhof, and M. Altmeyer. 2019. Phase separation of 53BP1 determines liquid-like behavior of DNA repair compartments. *EMBO J.* 38:e101379.

162. Beales, P.A., and T.K. Vanderlick. 2009. Partitioning of Membrane-Anchored DNA between Coexisting Lipid Phases. *J. Phys. Chem. B*. 113:13678–13686.

163. Rubio-Sánchez, R., S.E. Barker, M. Walczak, P. Cicuta, and L.D. Michele. 2021. A Modular, Dynamic, DNA-Based Platform for Regulating Cargo Distribution and Transport between Lipid Domains. *Nano Lett.* 21:2800–2808.

164. Bagheri, Y., A.A. Ali, P. Keshri, J. Chambers, A. Gershenson, and M. You. 2022. Imaging Membrane Order and Dynamic Interactions in Living Cells with a DNA Zipper Probe. *Angew. Chem. Int. Ed.* 61:e202112033.

165. Diamandis, E.P., and T.K. Christopoulos. 1991. The biotin-(strept)avidin system: principles and applications in biotechnology. *Clin. Chem.* 37:625–636.

166. Chiruvolu, S., S. Walker, J. Israelachvili, F.J. Schmitt, D. Leckband, and J.A. Zasadzinski. 1994. Higher order self-assembly of vesicles by site-specific binding. *Science*. 264:1753–1756.

167. Walker, S.A., and J.A. Zasadzinski. 1997. Electrostatic Control of Spontaneous Vesicle Aggregation. *Langmuir*. 13:5076–5081.

168. Momin, N., S. Lee, A.K. Gadok, D.J. Busch, G.D. Bachand, C.C. Hayden, J.C. Stachowiak, and D.Y. Sasaki. 2015. Designing lipids for selective partitioning into liquid ordered membrane domains. *Soft Matter*. 11:3241–3250.

169. You, K., Q. Huang, C. Yu, B. Shen, C. Sevilla, M. Shi, H. Hermjakob, Y. Chen, and T. Li. 2020. PhaSepDB: a database of liquid–liquid phase separation related proteins. *Nucleic Acids Res.* 48:D354–D359.

170. Ruff, K.M., S. Roberts, A. Chilkoti, and R.V. Pappu. 2018. Advances in Understanding Stimulus-Responsive Phase Behavior of Intrinsically Disordered Protein Polymers. *J. Mol. Biol.* 430:4619–4635.

171. Li, P., S. Banjade, H.-C. Cheng, S. Kim, B. Chen, L. Guo, M. Llaguno, J.V. Hollingsworth, D.S. King, S.F. Banani, P.S. Russo, Q.-X. Jiang, B.T. Nixon, and M.K. Rosen. 2012. Phase transitions in the assembly of multivalent signalling proteins. *Nature*. 483:336–340.

172. Bagheri, Y., M. Rouches, B.B. Machta, and S.L. Veatch. 2023. Experimental investigations of coupled polymer and membrane phase transitions. *Biophys. J.* 122:78a.